Interaction of the Benzenium Ion with Inert Ligands: IR Spectra of $C_6H_7^+$–L_n Cluster Cations (L = Ar, N_2, CH_4, H_2O)

Nicola Solcà and Otto Dopfer*[a]

Abstract: IR photodissociation spectra of mass-selected clusters composed of protonated benzene ($C_6H_7^+$) and several ligands L are analyzed in the range of the C–H stretch fundamentals. The investigated systems include $C_6H_7^+$–Ar, $C_6H_7^+$–$(N_2)_n$ ($n = 1-4$), $C_6H_7^+$–$(CH_4)_n$ ($n = 1-4$), and $C_6H_7^+$–H_2O. The complexes are produced in a supersonic plasma expansion using chemical ionization. The IR spectra display absorptions near 2800 and 3100 cm^{-1}, which are attributed to the aliphatic and aromatic C–H stretch vibrations, respectively, of the benzenium ion, that is, the σ complex of $C_6H_7^+$. The $C_6H_7^+$–$(CH_4)_n$ clusters show additional C–H stretch bands of the CH_4 ligands. Both the frequencies and the relative intensities of the $C_6H_7^+$ absorptions are nearly independent of the choice and number of ligands, suggesting that the benzenium ion in the detected $C_6H_7^+$–L_n clusters is only weakly perturbed by the microsolvation process. Analysis of photofragmentation branching ratios yield estimated ligand binding energies of the order of 800 and 950 cm^{-1} (≈9.5 and 11.5 kJ mol^{-1}) for N_2 and CH_4, respectively. The interpretation of the experimental data is supported by ab initio calculations for $C_6H_7^+$–Ar and $C_6H_7^+$–N_2 at the MP2/6-311G(2df,2pd) level. Both the calculations and the spectra are consistent with weak intermolecular π bonds of Ar and N_2 to the $C_6H_7^+$ ring. The astrophysical implications of the deduced IR spectrum of $C_6H_7^+$ are briefly discussed.

Keywords: arenium ions · aromatic substitution · cluster compounds · IR spectroscopy · reactive intermediates

Introduction

Protonation of aromatic molecules is a central process in organic chemistry and biology. Protonated aromatic molecules (AH^+) occur frequently as reactive intermediates in fundamental organic reaction mechanisms. For example, AH^+ may appear in the form of π complexes and/or σ complexes (Wheland intermediates) in electrophilic aromatic substitution reactions, which is one of the most common chemical reaction types for aromatic molecules.[1] It is well established that fundamental properties of these ion–molecule reactions, such as the structures and energies of minima and transition states, depend sensitively on the environment. Hence, gas-phase studies of AH^+ are required to separate their intrinsic molecular electronic properties from interfering solvation effects caused by counterions or surrounding solvent molecules.[2] In the past, nearly all experimental information about isolated AH^+ ions has come from mass spectrometry.[2] However, the results of these experiments provide only limited, indirect, and often disputable information about the details of the structure and energetics of AH^+ (e.g., the site of protonation).[2] In contrast to mass spectrometry, spectroscopic techniques (in particular IR spectroscopy) are very sensitive tools to probe directly the structure of molecules. Until very recently (2001), however, no spectroscopic characterization of the structure of any isolated AH^+ ion had been reported, mainly because of the experimental difficulties involved in the production of sufficient ion densities.

In the past two years, the application of two sensitive IR spectroscopic methods has provided the first structural characterization of basic AH^+ ions in the gas phase under controlled microsolvation conditions.[3–5] The first technique involves IR photodissociation (IRPD) spectroscopy of size-selected AH^+–L_n complexes, in which AH^+ is solvated by a well-defined number of inert ligands L (e.g., L = Ar or N_2).[3, 4, 5a] The IR spectrum of AH^+ is obtained by monitoring the laser-induced evaporation of the weakly bound ligand(s) through vibrational predissociation. The ligands L act as a messenger or spy,[6–9] because the perturbation of AH^+ upon complexation is small. The modest influence of the weak intermolecular interaction between AH^+ and L may either be controlled by the variation of L (i.e., the strength of the interaction) or determined by quantum chemical calculations.[3, 4, 6, 10, 11] So far, this strategy has been applied to AH^+–L_n complexes of protonated benzene ($C_6H_7^+$–L, L = Ar and N_2),[3] protonated phenol ($C_6H_7O^+$–Ar_n, $n = 1$ and 2),[4]

[a] Priv. Doz. Dr. O. Dopfer, Dr. N. Solcà
Institute for Physical Chemistry, University of Würzburg
Am Hubland, 97074 Würzburg (Germany)
Fax: (+49) 931-888-6378
E-mail: dopfer@phys-chemie.uni-wuerzburg.de

DOI: 10.1002/chem.200204629

and protonated fluorobenzene ($C_6H_6F^+$–$(N_2)_2$).[5a] IRPD spectra of $C_6H_7^+$–L in the C–H stretch range have unambiguously shown for the first time that the σ complex corresponds to the most stable structure of isolated $C_6H_7^+$ in agreement with condensed-phase data and ab initio calculations.[3] Thus, the long-standing controversy present in the mass spectrometry community, as to whether the σ or π complex is more stable, could be solved. Similarly, IRPD spectra of $C_6H_7O^+$–Ar_n in the O–H stretch range provided for the first time direct site-specific information about the preferred protonation sites of phenol in the gas phase.[4] Only σ complexes of $C_6H_7O^+$ are observed and protonation occurs preferentially in *ortho* and/or *para* position of the aromatic ring (carbenium ions) as well as at oxygen (oxonium ion). Protonation at the less favorable *meta* and *ipso* positions is not observed. As an alternative to IRPD of weakly bound AH^+–L_n clusters,[3, 4, 5a] the second approach utilizes IRPD of the bare AH^+ monomer. The latter technique enables the spectroscopic characterization of AH^+ completely free from any solvation effect (i.e., without messenger) and has so far been applied only to protonated fluorobenzene, $C_6H_6F^+$.[5b] In this study, the low dissociation energy of the fluoronium isomer of $C_6H_6F^+$ with respect to dehydrofluorination has been exploited to selectively record the IR spectrum of this specific isomer in the $C_6H_5^+$ fragment channel. The more stable carbenium isomers of $C_6H_6F^+$ escaped spectroscopic detection, because HF elimination requires much more energy for these ions. Very recently, several carbenium isomers of $C_6H_6F^+$ have been selectively identified through the application of the messenger approach to $C_6H_6F^+$–$(N_2)_2$.[5a]

Protonated benzene, the most simple arenium ion, is an ubiquitous ion in mass spectra of hydrocarbon molecules.[12] Moreover, it is a central species in modern models of the ion–molecule reaction chemistry of many terrestrial and extraterrestrial hydrocarbon plasmas, such as combustion flames,[13] planetary ionospheres,[14] and interstellar media.[15] Quantum chemical studies usually consider three binding sites for H^+ to C_6H_6.[3, 16, 17] All theoretical studies agree that the benzenium ion (σ complex, C_{2v}) corresponds to the global minimum on the potential of protonated benzene. The bridged structure (benzonium ion, C_{2v}) is identified as the lowest transition state between equivalent σ complexes, with an activation barrier of $E_a \approx 25-45\ kJ\,mol^{-1}$ for proton migration. The π complex (face-protonated structure, C_{6v}) is predicted to be a second order saddle point, lying approximately 200 $kJ\,mol^{-1}$ above the σ complex. Condensed phase spectroscopic (NMR, IR, UV)[18] and crystallographic data[19] of $C_6H_7^+$ in salts or super acid solutions are consistent with these theoretical predictions. Results of gas-phase studies to establish the most stable $C_6H_7^+$ structure free from solvation effects are controversial. The UV photodissociation spectrum of bare $C_6H_7^+$[20] differs significantly from the corresponding solution spectrum[18e] and does not provide any structural information. Mass spectrometric experiments offer only indirect and disputable structural data. Although most of these studies deduce that the σ complex is more stable than the π complex,[2a–d] a recent interpretation comes to the reverse conclusion.[2e]

In a recent communication,[3] IRPD spectra of $C_6H_7^+$–L (L = Ar, N_2) were analyzed in the C–H stretch range. The main results relevant for the present work are briefly summarized. The spectra of $C_6H_7^+$–Ar and $C_6H_7^+$–N_2 are very similar, confirming the expectation that the weakly bound ligands have indeed nearly no influence on the $C_6H_7^+$ properties. Comparison with the spectra calculated for the σ complex, the π complex, and the bridged structure of $C_6H_7^+$ unambiguously shows that the experimental spectra are clearly dominated by dimers of the σ complex. Consequently, the σ complex of $C_6H_7^+$ was concluded to be the most stable isomer of protonated benzene, in agreement with all calculations and most mass spectrometric conclusions. Preliminary ab initio calculations of the intermolecular potential-energy surfaces of $C_6H_7^+$–Ar and $C_6H_7^+$–N_2 suggested that the ligands are weakly attached to the aromatic ring (π bonds, Figure 1), with dissociation energies of only $D_e = 5.2$ and 11.1 $kJ\,mol^{-1}$, respectively.[3] As these energies are much smaller than the variations of the potential of bare $C_6H_7^+$,[21] the weak intermolecular π bonds cause only a negligible perturbation of the $C_6H_7^+$ properties, and the $C_6H_7^+$–L spectra closely resemble that of isolated $C_6H_7^+$.

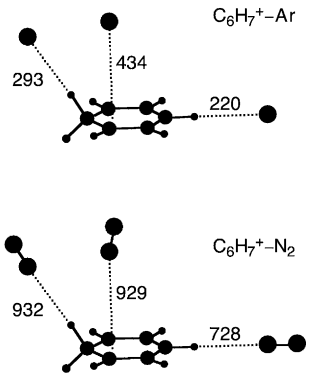

Figure 1. Sketch of the structures of selected minima on the intermolecular potential-energy surface of $C_6H_7^+$–L (L = Ar and N_2) calculated at the MP2/6-311G(2df,2pd) level. Intermolecular dissociation energies (D_e) are given in cm^{-1} (1 $kJ\,mol^{-1} \approx 83.6\ cm^{-1}$).

The present work reports IRPD spectra of a variety of isolated $C_6H_7^+$–L_n clusters (with L = Ar, N_2, CH_4, H_2O; $n \leq 4$) to extend the previous studies of $C_6H_7^+$–Ar and $C_6H_7^+$–N_2 to complexes with more strongly bound ligands and a larger number of solvent molecules. Hence, the results provide valuable information about the dependence of the $C_6H_7^+$ properties on both the degree of solvation and the intermolecular ion–solvent interaction strength. Eventually, controlled tuning of the microsolvation of AH^+ allows us to monitor step-by-step the transition from the gas to the condensed phase. Particularly for ion–molecule reaction mechanisms, strong solvation effects cause the properties of the gas-phase reaction to be very different from the condensed-phase analogue. For example, while the σ complex is the global minimum of isolated $C_6H_7^+$, it usually becomes a very reactive intermediate in electrophilic aromatic substitution reactions in solution. The IR spectroscopic approach is complemented by detailed calculations of the intermolecular potential of

$C_6H_7^+$–L (L = Ar, N_2) to investigate the interaction strength for various competing ligand binding sites (e.g., hydrogen bonds and π bonds, Figure 1). The calculated ligand binding energies will be compared to those derived from the analysis of the experimental photofragmentation branching ratios of larger $C_6H_7^+$–L_n clusters.

In general, gas-phase spectra of AH^+ are not only desired to characterize organic reaction mechanisms, but also to identify such ions in hydrocarbon plasmas, such as combustion flames and interstellar media. For example, protonated polycyclic aromatic hydrocarbon molecules are important ions in modern astrochemical models[15] and discussed as possible carriers for the well known but not yet assigned diffuse interstellar bands (DIBs) as well as the unidentified IR emission bands (UIR).[15b, 22] The recent detection of benzene in interstellar objects supports the suggestion of the presence of (protonated) aromatic molecules in interstellar space.[22] The astrochemical implications of the deduced IR spectrum of $C_6H_7^+$ will be briefly discussed.

Experimental Section

IRPD spectra of $C_6H_7^+$–L_n (L = Ar, N_2, CH_4, H_2O) clusters were recorded in a tandem mass spectrometer, which was coupled to an ion source and an octopole ion trap.[23] The ion source combines electron ionization with a pulsed supersonic expansion. The expanding gas mixture was produced by passing a suitable carrier gas at room temperature through a reservoir filled with benzene. The employed gas composition was H_2:He:Ar (ratio 1:1:16, 10 bar stagnation pressure) for the production of $C_6H_7^+$–Ar, H_2:He:N_2 (1:1:20, 10 bar) for $C_6H_7^+$–$(N_2)_n$, and H_2:He:CH_4 (1:1:16, 6 bar) for $C_6H_7^+$–$(CH_4)_n$. The expansion gas for the generation of the $C_6H_7^+$–H_2O dimer was produced by passing a H_2:He:N_2 mixture (1:1:16, 6 bar) through two successive reservoirs filled with water and benzene. Electron ionization of the expansion ($E = 10^2$ eV) close to the nozzle orifice and subsequent ion–molecule and clustering reactions in the high-pressure regime of the expansion generated cold $C_6H_7^+$–L_n cluster ions. The dominant mechanism for $C_6H_7^+$–L_n production begins with chemical ionization of C_6H_6 (generating $C_6H_7^+$) and is followed by three-body aggregation reactions to form weakly bound $C_6H_7^+$–L_n.[3] A typical mass spectrum of the ion source is shown in Figure 2 for the conditions used for $C_6H_7^+$–Ar generation. The mass spectrum is dominated by (protonated) benzene cluster ions, their fragments, and ArH_n^+ ($n = 0, 1$). Major fragment ions of $C_6H_{6/7}^+$ are indicated by filled circles.[12] The relative abundance of $C_6H_7^+$–Ar (open circle) with respect to $C_6H_7^+$ was only 1:1400. The small efficiency for cluster formation under optimized conditions is in line with the weak interaction between $C_6H_7^+$ and Ar.

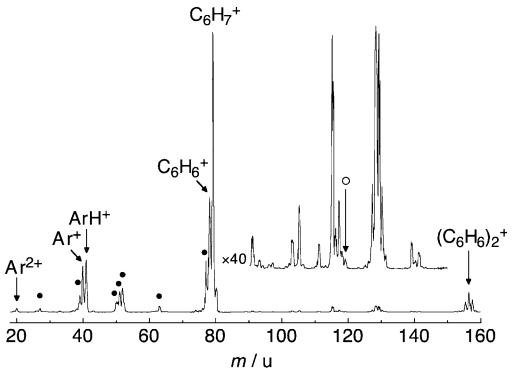

Figure 2. Mass spectrum of the cluster ion source under the conditions used for the production of $C_6H_7^+$–Ar. The spectrum is dominated by (protonated) benzene cluster ions, their fragments, and ArH_n^+ ($n = 0, 1$). Major fragment ions of $C_6H_{6/7}^+$ are indicated by filled circles.[12] Part of the spectrum is vertically expanded by a factor of 40 to show weak peaks. The relative intensities of $C_6H_7^+$–Ar (open circle) and $C_6H_7^+$ are 1:1400.

The generated $C_6H_7^+$–L_n ions were selected by an initial quadrupole mass spectrometer (QMS1) and interacted in an adjacent octopole ion guide with a tunable IR laser pulse generated by an optical parametric oscillator laser system. Resonant vibrational excitation of $C_6H_7^+$–L_n led to the evaporation of weakly bound ligands [Eq. (1)]:

$$C_6H_7^+\text{–}L_n + \nu_{IR} \longrightarrow C_6H_7^+\text{–}L_m + (n-m)L \quad (1)$$

Only the rupture of the weak intermolecular bonds was observed upon laser excitation. The $C_6H_7^+$–L_m fragment ions were selected by a second quadrupole mass filter (QMS2) and monitored as a function of the laser frequency to obtain the IRPD spectrum of $C_6H_7^+$–L_n. In addition to laser-induced dissociation (LID), $C_6H_7^+$–L_m fragment ions could also be produced by metastable decay (MD) of hot parent ions in the octopole region. To distinguish LID signals from MD background, the ion source was triggered at twice the laser repetition rate and signals from alternating triggers were subtracted. As an example, Figure 3 shows the mass spectra

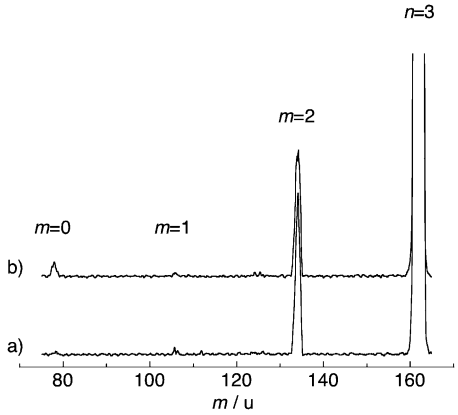

Figure 3. Mass spectra obtained by mass-selecting $C_6H_7^+$–$(N_2)_3$ with QMS1 and scanning QMS2 without (a) and with (b) resonant laser excitation. In spectrum a the $C_6H_7^+$–$(N_2)_m$ fragment ions ($m = 1, 2$) arise from metastable decay. In spectrum b, the laser is tuned to a resonance of $C_6H_7^+$–$(N_2)_3$, $\nu_{IR} = 2827$ cm^{-1}, leading to additional fragmentation into the $C_6H_7^+$ channel ($m = 0$).

obtained by mass selecting $C_6H_7^+$–$(N_2)_3$ with QMS1 and scanning QMS2 without (a) and with resonant laser excitation (b). Spectrum a contains a strong parent peak ($n = 3$) and weak signals in the $m = 2$ and $m = 1$ fragment channels arising from MD (3% and 0.07% of parent). Spectrum b, obtained with the laser tuned to a resonance of $C_6H_7^+$–$(N_2)_3$, reveals additional fragmentation into the $m = 0$ channel caused by LID (0.3% of parent). In this case, excitation occurred at $\nu_{IR} = 2\sigma_{C-C}$ (2827 cm^{-1}), which was the strongest transition observed in the investigated spectral range. The weak photodissociation yield of 0.3% of the parent ions implies that all observed transitions have rather low IR oscillator strengths, giving rise to the modest signal-to-noise ratios. This observation confirms previous experience that C–H stretch vibrations of aromatic cations have low IR intensities.[8, 24] According to Equation (1), several fragment channels (m) may be observed for parent clusters with $n \geq 2$. In this case, action spectra were recorded simultaneously in the two dominant fragment channels. As the spectra recorded in different daughter channels are similar, only the spectrum obtained in the dominant channel is shown in the figures.

Pulsed and tunable IR laser radiation was created by a single-mode optical parametric oscillator pumped by a Nd:YAG laser. The laser pulses are characterized by a bandwidth of 0.02 cm^{-1}, a duration of 5 ns, and an intensity of < 200 kW cm^{-2}. Calibration of the laser frequency (accurate to better than 0.2 cm^{-1}) was facilitated by optoacoustic reference spectra of HDO recorded simultaneously with the action spectra.[25]

Results and Discussion

Computational results: Quantum chemical calculations for $C_6H_7^+$ and $C_6H_7^+$–L (L = Ar, N_2) were carried out at the MP2/6-311G(2df,2pd) level of theory.[26] All coordinates were allowed to relax during the search for stationary points. Intermolecular interaction energies of the dimers were fully counter-poise corrected for basis set superposition error.[27] Previous calculations for the $C_6H_7^+$ monomer at this level of theory confirmed that the σ complex corresponds to the global minimum structure on the intramolecular potential-energy surface, whereas the bridged structure (transition state) and the π complex (saddle point) were predicted to be 27 and 206 kJ mol^{-1} higher in energy, respectively.[3] Consequently, only $C_6H_7^+$–L dimer structures with a σ complex of $C_6H_7^+$ are considered in the present work. Figure 1 summarizes the calculated structures of selected $C_6H_7^+$–L minima. Three principal binding sites are identified on the intermolecular $C_6H_7^+$–L potential for L = Ar and N_2. The ligand can bind to the π-electron system of the aromatic ring (π bond) or form hydrogen bonds to either the aliphatic CH_2 group (CH_2 bond) or an aromatic CH bond (CH bond). For CH-bonding, only the *para* position with respect to the CH_2 group is considered, because the interaction with other CH bonds is expected to be very similar (Figure 1). The analysis of the charge distribution in $C_6H_7^+$, employing the AIM (atoms-in-molecules) population analysis, yields a larger positive partial charge on the CH_2 protons (+0.16 e) compared to any of the CH protons (+0.12 e), suggesting that the former protons are more acidic. This view is supported by the averaged lengths and harmonic vibrational stretching frequencies of the C–H bonds in $C_6H_7^+$, which confirm that the aliphatic C–H bonds are indeed weaker and longer than the aromatic ones: $r_e \approx$ 1.10 versus 1.08 Å and $\omega_{CH} \approx 3000$ versus 3250 cm^{-1} for CH_2 versus CH, respectively.

In the case of $C_6H_7^+$–Ar, the π-bound structure with C_s symmetry is the global minimum on the intermolecular potential, with a dissociation energy of $D_e = 434$ cm^{-1} and an intermolecular Ar–ring separation of $R_e = 3.37$ Å. The Ar ligand is shifted from the center of the aromatic ring toward the CH_2 group. The structure with the nearly linear hydrogen bond to the CH_2 group is a local minimum (C_s) with $D_e =$ 293 cm^{-1} and an Ar–H separation of $R_e = 2.65$ Å. The other local H-bound minimum features a linear and slightly weaker hydrogen bond to the CH bond in the *para* position (C_{2v}) with $D_e = 220$ cm^{-1} and $R_e = 2.78$ Å. Apparently, for $C_6H_7^+$–Ar the dispersion interaction (favoring the π bond) overrides the induction interaction (favoring the hydrogen bonds).

The interaction in $C_6H_7^+$–N_2 is significantly stronger than in $C_6H_7^+$–Ar, because the nonvanishing quadrupole moment of N_2 (-5×10^{-40} C m^2)[28] gives rise to additional electrostatic attraction, mainly through charge–quadrupole interactions. Both dispersion and induction forces are also expected to be slightly stronger in $C_6H_7^+$–N_2, as the (parallel) polarisability of N_2 is larger than that of Ar ($\alpha = 1.64$ and 2.38 Å^3 for Ar and N_2, respectively).[28] The anisotropy of the long-range charge-induced dipole and charge–quadrupole interaction favors a linear over a T-shaped approach of N_2 toward a positive charge.[6, 10a, 29–31] Consequently, all three $C_6H_7^+$–N_2 minima in Figure 1 feature (nearly) linear $C_6H_7^+$–N–N configurations (i.e., the N_2 molecule is pointing toward the cation). In contrast to $C_6H_7^+$–Ar, the $C_6H_7^+$–N_2 minima with the π bond ($D_e = 929$ cm^{-1}, $R_e = 3.04$ Å, C_s) and the hydrogen bond to the CH_2 group ($D_e = 932$ cm^{-1}, $R_e = 2.29$ Å, C_s) are very similar in energy. Again, the linear hydrogen bond to the CH bond ($D_e = 728$ cm^{-1}, $R_e = 2.43$ Å, C_{2v}) is weaker than that to the CH_2 group. Apparently, while in $C_6H_7^+$–Ar the π bond is clearly more stable than the hydrogen bonds (by 50–100%), the additional electrostatic and induction interactions in $C_6H_7^+$–N_2 cause the hydrogen bonds to become more similar in energy to the π bond. In line with the larger proton affinity of N_2 compared to Ar (494 and 369 kJ mol^{-1}),[32] the hydrogen bonds gain more in stability than the π bonds by passing from Ar to N_2.

In general, the long-range attraction of the intermolecular potential in weakly hydrogen-bound ion–ligand complexes of the type AH^+–L is dominated by the electrostatic and inductive forces between the charge distribution of AH^+ and the permanent multipole moments and polarizabilities of L.[6, 10, 33] A key factor for the interaction strength is thus the positive partial charge localized on the intermediate proton (q_H). Table 1 and Figure 4 summarize the calculated binding energies (D_e) for a variety of hydrogen-bound AH^+–L dimers (L = Ar, N_2) involving aromatic cations, namely $C_6H_7^+$ and the cyclopropenyl (*c*-$C_3H_3^+$), aniline ($C_6H_7N^+$), and (protonated) phenol ($C_6H_{6/7}O^+$) cations. As a general trend, D_e increases with q_H. In particular, the CH_2–L bonds are much weaker than the OH–L and NH_2–L bonds. As mentioned earlier, the CH–L bonds in $C_6H_7^+$–L are weaker than the CH_2–L bonds, because the CH protons are less acidic.

Table 1. Dissociation energies (D_e) of selected hydrogen-bound AH^+–Ar and AH^+–N_2 dimers involving aromatic AH^+ ions, along with the positive partial charge (AIM) on the intermediate proton (q_H), calculated at the MP2/6-311G(2df,2pd) level (1 kJ mol$^{-1} \approx$ 83.6 cm^{-1}).

AH^+	q_H [e]	D_e (Ar) [cm^{-1}]	D_e (N_2) [cm^{-1}]
$C_6H_7^+$ (CH)	0.12	220	728
$C_6H_7^+$ (CH_2)	0.16	293	932
c-$C_3H_3^+$ (CH)[a]	0.27	365	1227
$C_6H_7N^+$ (NH_2)[b]	0.48	513	1431
$C_6H_7O^+$ (OH)[c]	0.67	633	1808
$C_6H_6O^+$ (OH)[d]	0.66	656	1910

[a] Ref. [29]. [b] Refs. [31, 46]. [c] Ref. [54] (assuming *para* protonation). [d] Refs. [30, 54].

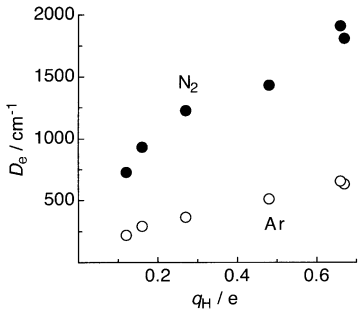

Figure 4. Dissociation energies (D_e) of selected H-bound AH^+–Ar and AH^+–N_2 dimers involving aromatic AH^+ ions as a function of the positive partial charge (AIM) on the intermediate proton (q_H), calculated at the MP2/6-311G(2df,2pd) level (Table 1).

Spectroscopic results: The IRPD spectra of the $C_6H_7^+$–L dimers (L = Ar, N_2, CH_4, H_2O) recorded in the C–H stretch range are reproduced in Figure 5, along with a simulation of the spectrum calculated for the σ complex of the $C_6H_7^+$ monomer. The corresponding spectra of larger $C_6H_7^+$–$(N_2)_n$ and $C_6H_7^+$–$(CH_4)_n$ clusters with $n \leq 4$ are compared in Figure 6. The positions, widths, and assignments of the observed transitions (labeled A – H) are listed in Table 2. The assignments of the $C_6H_7^+$–Ar/N_2 spectra have been discussed previously.[3] Thus, only the results relevant for the present work are briefly summarized here.

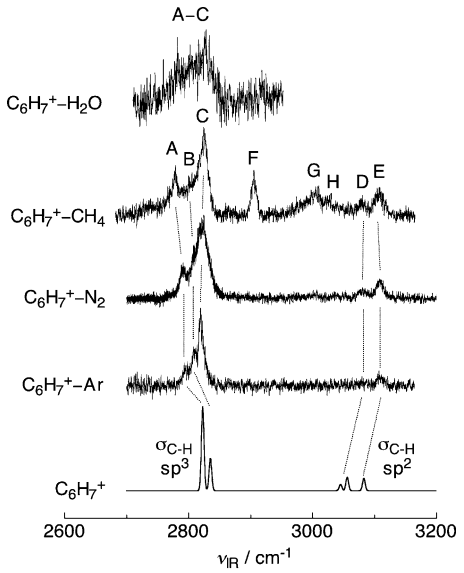

Figure 5. IRPD spectra of $C_6H_7^+$–L (L = Ar, N_2, CH_4, H_2O) in the C–H stretch range recorded in the $C_6H_7^+$ fragment channel. The positions, widths, and assignments of the observed transitions (labeled A – H) are listed in Table 2. The experimental spectra are compared to a spectrum of the σ complex of isolated $C_6H_7^+$ calculated at the MP2/6-31G(2df,2pd) level (convolution width 5 cm^{-1}, scaling factor 0.9426).[3] Aromatic C–H stretch modes (σ_{C-H}, sp^2) occur near 3100 cm^{-1}, whereas aliphatic C–H stretch modes appear near 2800 cm^{-1} (σ_{C-H}, sp^3). Corresponding transitions are connected by dotted lines.

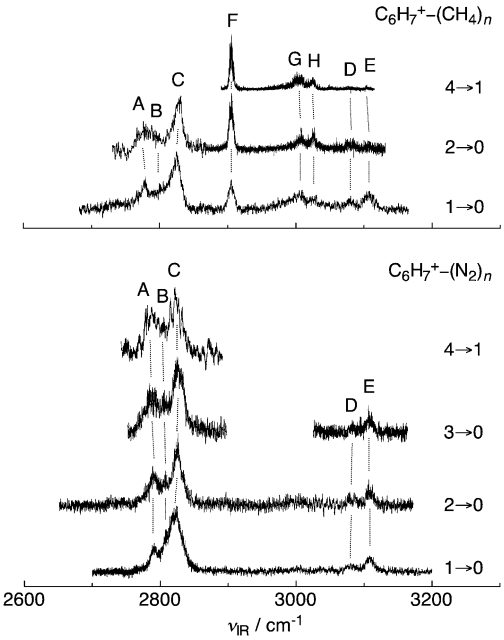

Figure 6. IRPD spectra of $C_6H_7^+$–L_n with L = N_2 and CH_4 recorded in the dominant $C_6H_7^+$–L_m fragment channel (indicated as $n \rightarrow m$). The positions, widths, and assignments of the observed transitions (labeled A – H) are listed in Table 2. Corresponding transitions are connected by dotted lines.

$C_6H_7^+$–L (L = Ar, N_2, CH_4): The IRPD spectra of $C_6H_7^+$–Ar/N_2 reveal five transitions in the C–H stretch range (A – E). By comparison with the spectrum calculated for the σ complex of $C_6H_7^+$, bands A and B near 2800 cm^{-1} have been

Table 2. Band maxima and widths (FWHM in parentheses) of the transitions [in cm^{-1}] observed in the IRPD spectra of $C_6H_7^+$–L_n recorded in the dominant fragment channel.

L	*n*	peak	position	assignment	L	*n*	peak	position	assignment
Ar	1[a]	A	2795 (6)	sym σ_{C-H} (sp^3)	CH_4	1	A	2778 (8)	sym σ_{C-H} (sp^3)
		B	2810 (8)	asym σ_{C-H} (sp^3)			B	2803 (7)	asym σ_{C-H} (sp^3)
		C	2819 (8)	$2\sigma_{C-C}$ (sp^2)			C	2825 (14)	$2\sigma_{C-C}$ (sp^2)
		E	3110 (10)	σ_{C-H} (sp^2)			F	2906 (10)	ν_1
N_2	1[a]	A	2792 (9)	sym σ_{C-H} (sp^3)			G	3005 (24)	ν_3
		B	2809 (6)	asym σ_{C-H} (sp^3)			H	3026 (14)	ν_3
		C	2821 (15)	$2\sigma_{C-C}$ (sp^2)			D	3080 (14)	σ_{C-H} (sp^2)
		D	3081 (14)	σ_{C-H} (sp^2)			E	3108 (20)	σ_{C-H} (sp^2)
		E	3109 (12)	σ_{C-H} (sp^2)		2	A	2776 (15)	sym σ_{C-H} (sp^3)
	2	A	2791 (15)	sym σ_{C-H} (sp^3)			B	2795 (10)	asym σ_{C-H} (sp^3)
		B	2808 (8)	asym σ_{C-H} (sp^3)			C	2829 (14)	$2\sigma_{C-C}$ (sp^2)
		C	2825 (13)	$2\sigma_{C-C}$ (sp^2)			F	2905 (7)	ν_1
		D	3083 (15)	σ_{C-H} (sp^2)			G	3008 (10)	ν_3
		E	3109 (12)	σ_{C-H} (sp^2)			H	3025 (7)	ν_3
	3	A	2788 (18)	sym σ_{C-H} (sp^3)			D	3081 (14)	σ_{C-H} (sp^2)
		B	2806 (12)	asym σ_{C-H} (sp^3)			E	3107 (11)	σ_{C-H} (sp^2)
		C	2827 (16)	$2\sigma_{C-C}$ (sp^2)		4	F	2905 (5)	ν_1
		D	3083 (12)	σ_{C-H} (sp^2)			G	3004 (17)	ν_3
		E	3109 (10)	σ_{C-H} (sp^2)			H	3025 (7)	ν_3
	4	A	2789 (11)	sym σ_{C-H} (sp^3)			D	3078 (11)	σ_{C-H} (sp^2)
		B	2807 (13)	asym σ_{C-H} (sp^3)			E	3105 (6)	σ_{C-H} (sp^2)
		C	2826 (20)	$2\sigma_{C-C}$ (sp^2)	H_2O	1	A/B	2797 (36)	σ_{C-H} (sp^3)
							C	2826 (23)	$2\sigma_{C-C}$ (sp^2)

[a] Ref. [3].

assigned to the symmetric and antisymmetric C–H stretch modes of the aliphatic CH_2 group (sp^3 hybridization of the C atom). The third and most intense transition in this frequency range (band C) has been interpreted as a C–C stretch overtone of the ring, $2\sigma_{C-C}(sp^2)$, on the basis of spectra of isotopically labeled complexes, $C_6H_{7-x}D_x^+$–Ar/N_2.[3] This transition is not included in the simulation of $C_6H_7^+$ in Figure 5. Two additional bands (D and E) occur with significantly lower intensity in the 3100 cm^{-1} range. Those are readily assigned to aromatic C–H stretch modes of the ring (sp^2 hybridization of the C atom),[3] and occur close to the corresponding transitions of $C_6H_6^+$–L (near 3095 cm^{-1}).[8, 34]

Similar to $C_6H_7^+$–Ar/N_2, the $C_6H_7^+$–CH_4 spectrum shows the five transitions attributed to absorptions of the $C_6H_7^+$ core (A–E). Moreover, the $C_6H_7^+$–CH_4 spectrum demonstrates additional bands at 2906 (F), 3005 (G), and 3026 cm^{-1} (H) that are not present in the $C_6H_7^+$–Ar/N_2 spectra. Consequently, they are assigned to transitions of the CH_4 ligand. By comparison with the bare CH_4 spectrum, they can be attributed to the symmetric and antisymmetric C–H stretch fundamentals of the dimer ($\nu_1 = 2916.5\ cm^{-1}$ and $\nu_3 = 3019.5\ cm^{-1}$ for isolated CH_4).[35] The presence of $C_6H_7^+$ has a profound effect on both the IR intensities and the frequencies of the CH_4 vibrations. For example, the IR-forbidden ν_1 fundamental of tetrahedral CH_4 becomes comparable in intensity to the strongly IR-active ν_3 fundamental in $C_6H_7^+$–CH_4. The presence of the charge polarizes the CH_4 molecule, giving rise to the strong IR enhancement of ν_1. In addition, the ν_1 frequency is reduced by 11 cm^{-1} upon complexation with $C_6H_7^+$, implying that the intermolecular interaction increases slightly upon ν_1 excitation. The ν_3 fundamental is triply degenerate for isolated CH_4. Symmetry reduction splits ν_3 into at least two components in $C_6H_7^+$–CH_4 (bands G and H) with a separation of 21 cm^{-1}. In general, the effects of $C_6H_7^+$ on the vibrational spectrum of CH_4 are very similar to those observed and discussed in more detail previously for the related $C_6H_6^+$–CH_4 dimer.[8a]

The C–H stretch bands of the aliphatic CH_2 group near 2800 cm^{-1} (A and B), together with the $2\sigma_{C-C}$ overtone (band C), are an unambiguous spectroscopic fingerprint of the σ complex of $C_6H_7^+$.[3] Other $C_6H_7^+$ structures, such as the π complex or the bridged structure, are not expected to absorb in the 2800 cm^{-1} range.[3] Consequently, the $C_6H_7^+$–L dimers with L = Ar, N_2, and CH_4 are concluded to have a σ complex of $C_6H_7^+$ as the cation core. Thus, the proton is clearly attached to C_6H_6 and not to the ligand L, implying that the observed $[C_6H_6$–$L]H^+$ complexes are indeed best described by $C_6H_7^+$–L and not by C_6H_6–LH^+. This view is supported by the large disparity in the proton affinities (PA) of C_6H_6 (PA = 750 kJ mol^{-1}) and L (PA = 369, 494, and 544 kJ mol^{-1} for Ar, N_2, and CH_4).[32] Moreover, in all three cases only $C_6H_7^+$ is observed as fragment ion upon IR excitation. For $C_6H_7^+$–CH_4, absorptions of the CH_4 ligand are clearly identified and confirm the $C_6H_7^+$–CH_4 notation (the IR spectra of CH_5^+[36] and its clusters[37] are rather different from that of CH_4). In addition, C_6H_6–LH^+ complexes are expected to absorb near the C–H stretch fundamentals of neutral C_6H_6 ($3061 \pm 13\ cm^{-1}$),[38] but no signal is observed in the experimental spectra in this range (Figure 5).

All spectroscopic, thermodynamic, and theoretical data for $C_6H_7^+$–L with L = Ar, N_2, and CH_4 clearly suggest that their most stable structures are composed of $C_6H_7^+$ and L. The interaction between $C_6H_7^+$ and L is expected to increase in the order $Ar < N_2 < CH_4$ on the basis of the proton affinities, polarizabilities, and higher order permanent multipole moments of L. The theoretical results in Figure 1 confirm this conclusion. Despite the somewhat different binding energies, the IRPD spectra of $C_6H_7^+$–L are quite similar in the C–H stretch range. The differences between the center frequencies of bands A–E of $C_6H_7^+$–L ($\leq 17\ cm^{-1}$) are of the order of the widths of the bands (6–20 cm^{-1}). This observation implies that the perturbation of L on the $C_6H_7^+$ spectrum is relatively weak in the C–H stretch range, and the observed cluster spectra provide good approximations of the IR spectrum of bare $C_6H_7^+$ (messenger technique).[3]

Closer inspection actually shows that the frequencies of bands A–E display small but noticeable monotonic shifts as the interaction increases in the order $Ar < N_2 < CH_4$ (Table 2, Figure 7): the shifts are largest for band A (−17 cm^{-1}),

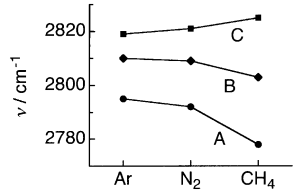

Figure 7. The positions of the bands A, B, and C observed in the IRPD spectra of $C_6H_7^+$–L are plotted as a function of the ligand L. The monotonic trends suggest that the intermolecular interaction increases in the order $Ar < N_2 < CH_4$.

smaller for B (−7 cm^{-1}) and C (+6 cm^{-1}), and almost negligible for D (−1 cm^{-1}) and E (−2 cm^{-1}). Small shifts of C–H and C–C stretch vibrations are expected for $C_6H_7^+$–L structures in which L forms a π bond to the $C_6H_7^+$ ring. Indeed, the π-bound isomer is calculated to be the most stable structure for $C_6H_7^+$–Ar (Figure 1). For $C_6H_7^+$–N_2, both the π-bound and CH_2-bound structures are predicted to have very similar stabilization energies ($D_e \approx 930\ cm^{-1}$). However, the calculations are expected to somewhat underestimate the dispersion forces and thus the binding energy of the π-bound isomer (whereas the hydrogen bond should be described more accurately). Both $C_6H_7^+$–N_2 structures can clearly be distinguished by the frequencies of the symmetric C–H stretch of the CH_2 group (band A). The calculations predict a large red shift of the order of 50 cm^{-1} and high IR intensity for this mode in the CH_2-bound structure (i.e., it should occur near 2750 cm^{-1}) and a much smaller shift for the π-bound isomer (+3 cm^{-1}).[39] The experimental $C_6H_7^+$–N_2 spectrum lacks absorptions between 2650 and 2780 cm^{-1}, suggesting that π-bound $C_6H_7^+$–N_2 is the dominant isomer in the supersonic expansion and significantly more stable than the CH_2-bound structure. Similar conclusions apply also to $C_6H_7^+$–CH_4. The fact that the CH_4 transitions of $C_6H_7^+$–CH_4 are both in frequency and intensity very similar to the bands of the π-bound $C_6H_6^+$–CH_4 dimer also supports a π-bound $C_6H_7^+$–CH_4 structure.[8a] Actually, band A is most sensitive to the variation

of L (from all observed transitions, Figure 7), suggesting that L is interacting weakly with one proton of the CH_2 group of $C_6H_7^+$. This interpretation is supported by the π-bound structures of $C_6H_7^+$–Ar/N_2 (Figure 1), in which L is slightly attracted by the CH_2 group (possibly through some weak and largely nonlinear hydrogen bond). Hence, all available spectroscopic and theoretical information for $C_6H_7^+$–L with L = Ar, N_2, and CH_4 are in line with π-bound global minima on the intermolecular potentials.

$C_6H_7^+$–H_2O: Interestingly, the part of the $C_6H_7^+$–H_2O spectrum recorded in the present work (Figure 5) also reveals resonant broad absorptions in the 2800 cm^{-1} range (bands A – C), suggesting that the observed complex has also an H_2O ligand attached to a $C_6H_7^+$ core. At first glance, the $[C_6H_6–H_2O]H^+$ complex is expected to have a $C_6H_7^+$–H_2O structure, because the PA of C_6H_6 (750 kJ mol^{-1}) is larger than that of H_2O (691 kJ mol^{-1}).[32] However, a recent theoretical study at the MP2/6-31 + G(d,p) level predicts the $C_6H_7^+$–H_2O structure to be slightly higher in energy than the C_6H_6–H_3O^+ complex (by 11 kJ mol^{-1}).[40] The C_6H_6–H_3O^+ complex, featuring a π hydrogen bond of a proton of H_3O^+ to the aromatic C_6H_6 ring, has a calculated dissociation energy of 97 kJ mol^{-1} with respect to the $C_6H_6 + H_3O^+$ limit. On the other hand, the $C_6H_7^+$–H_2O structure with a hydrogen bond of H_2O to the CH_2 group of $C_6H_7^+$ is stabilized by only 42 kJ mol^{-1} with respect to the $C_6H_7^+ + H_2O$ limit. Hence, although the $C_6H_7^+ + H_2O$ limit is lower than $C_6H_6 + H_3O^+$ (by $PA_{C_6H_6} - PA_{H_2O} = 59$ kJ mol^{-1}),[32] C_6H_6–H_3O^+ appears to be slightly more stable than $C_6H_7^+$–H_2O. Both $[C_6H_6–H_2O]H^+$ structures can possibly be formed in the plasma expansion of C_6H_6, H_2O, He, N_2, and H_2. Assuming that the spectral features observed in the IRPD spectrum correspond indeed to bands A – C of $C_6H_7^+$ (as indicated in Figure 5 and Table 2), the $[C_6H_6–H_2O]H^+$ complex detected in the present work has the $C_6H_7^+$–H_2O type structure, confirming that this complex is at least a minimum on the $[C_6H_6–H_2O]H^+$ potential. Similar to $C_6H_7^+$–L (L = Ar, N_2, CH_4), several isomeric structures may exist for $C_6H_7^+$–H_2O (Figure 1).[34] As only a short part of the $C_6H_7^+$–H_2O spectrum has been obtained in this preliminary study on $[C_6H_6–H_2O]H^+$, it is difficult to infer definitive experimental information about the relative stability of possible isomers. Higher level calculations and additional spectroscopic data are required to investigate further details of the important $[C_6H_6–H_2O]H^+$ potential. The following two observations are in line with the thermochemical predictions that the $C_6H_7^+ + H_2O$ limit is lower in energy than $C_6H_6 + H_3O^+$. All photodissociation signals of $[C_6H_6–H_2O]H^+$ are observed in the $C_6H_7^+$ fragment ion channel (no signal is detected in the H_3O^+ channel). In addition, low-energy collision-induced dissociation[41] of $[C_6H_6–H_2O]H^+$ yields 99.6 % $C_6H_7^+$ and only 0.4 % H_3O^+ fragment ions.

The dissociation energy of $C_6H_7^+$–H_2O is clearly much larger than that of the other $C_6H_7^+$–L (L = Ar, N_2, CH_4) dimers, mainly because of the additional charge – dipole interaction. Hence, the effective cooling in the expansion is less efficient for the former complex.[42] In addition, cold $C_6H_7^+$–L (L = Ar, N_2, CH_4) dimers can readily be dissociated by single photon absorption from the ground vibrational state (as $\nu_{IR} > D_0$). In contrast, fragmentation of the much more strongly bound $C_6H_7^+$–H_2O dimer probably requires a certain amount of internal excitation prior to IR absorption because D_0 is likely to be larger than ν_{IR} (only single photon absorption processes can be observed for the maximal available laser intensities of 200 kW cm^{-2}).[5, 34a] Thus, only sequence hot bands originating from excited vibrational states can be observed for $C_6H_7^+$–H_2O, leading to both broader band contours and lower dissociation yields compared to the other $C_6H_7^+$–L dimers (Figure 5, Table 2).

Larger $C_6H_7^+$–L_n clusters: The IRPD spectra of $C_6H_7^+$–L_n (L = N_2 and CH_4, $n \leq 4$) in Figure 6 show only minor changes as n increases (Table 2). All spectra display the absorptions characteristic for the $C_6H_7^+$ ion core (A – E), suggesting that the proton still resides on the C_6H_6 moiety. Consequently, intracluster proton transfer to the solvent is not observed for the cluster size range investigated. This result is in line with the large difference in the PA of C_6H_6 and L. For AH^+–L_n clusters with a smaller difference $\Delta PA_{A–L}$, proton transfer from A to the solvent clusters L_n is often observed when n exceeds a certain threshold.[43] The bands F – H assigned to CH_4 absorptions of $C_6H_7^+$–$(CH_4)_n$ are nearly independent of n with respect to both frequency and relative intensity. Moreover, the widths tend to decrease as n increases. Both observations imply that there is little interaction between the CH_4 ligands within the $C_6H_7^+$–$(CH_4)_n$ cluster. A similar situation was recently observed for the corresponding $C_6H_6^+$–$(CH_4)_n$ clusters.[8a] As n increases, the relative intensities of CH_4 transitions (F – H) increase relative to those of $C_6H_7^+$ (A – E), simply because the number of CH_4 chromophores in the cluster increases.

Table 3 summarizes the photofragmentation branching ratios measured for resonant excitation of $C_6H_7^+$–L_n [see Eq. (1)]. The laser is tuned to transition C (≈2825 cm^{-1}) for L = N_2 and F (≈2905 cm^{-1}) for L = CH_4. In agreement with previous studies on related systems,[8a, 11, 23, 29b, 31, 44] the range of fragment channels (m) observed for a given parent cluster (n) is rather narrow: the photodissociation signal is observed in one or two major channels. This information can be used to estimate ligand binding energies within the framework of a simple model.[8a, 11, 23, 29b, 31, 44] For this purpose, it is supposed that the absorbed photon energy (ν_{IR}) is available for ligand evaporation. Moreover, all ligands are assumed to be equivalent, with (roughly) the same dissociation energy. For $C_6H_7^+$–$(N_2)_n$, the photon energy of ≈2825 cm^{-1} is sufficient for the evaporation of approximately 3.5 N_2 ligands, yielding

Table 3. Photofragmentation branching ratios [in %] of $C_6H_7^+$–L_n for the photoinduced reaction in Equation (1).[a]

L	n	$m = 0$	$m = 1$	$m = 2$
N_2	1 – 3	100		
	4	50	50	
	5		60	40
CH_4	1,2	100		
	4	15	85	

[a] Measured for bands C and F for L = N_2 and CH_4, respectively. Only channels contributing more than 5 % are listed. Uncertainties are estimated as 10 %.

an averaged ligand binding energy of the order of $D_0 \approx 800\ cm^{-1}$. This value is compatible with the calculated dissociation energy of $D_e \approx 930\ cm^{-1}$ (Figure 1). For $C_6H_7^+$–$(CH_4)_4$, the photon energy of $\approx 2905\ cm^{-1}$ leads to the evaporation of predominantly $3\,CH_4$ ligands, yielding a rough averaged ligand binding energy of the order of $D_0 \approx 950\ cm^{-1}$. Thus, the photofragmentation data suggest that the $C_6H_7^+$–CH_4 interaction is only slightly stronger than the $C_6H_7^+$–N_2 interaction.

It is illustrative to compare the derived $C_6H_7^+$–L binding energies with those of other π-bound A^+–L complexes involving related aromatic A^+ ions, such as benzene ($C_6H_6^+$),[8a,d] phenol ($C_6H_6O^+$)[11, 30, 45] aniline ($C_6H_7N^+$),[9, 31, 46] and cyclopropenyl (c-$C_3H_3^+$),[29] which have been investigated with similar spectroscopic and theoretical techniques (Table 4). In line with the increasing polarizabilities, the binding energies of the intermolecular π bonds increase in the order $Ar < N_2 < CH_4$. Moreover, the dissociation energies are comparable for the same ligand and different aromatic cations. They are of the order of $500\ cm^{-1}$ for A^+–Ar, around $800\ cm^{-1}$ for A^+–N_2, and $\approx 1000\ cm^{-1}$ for A^+–CH_4. The comparison in Table 4 suggests that the binding energy for $C_6H_6^+$–N_2 of $\approx 330-550\ cm^{-1}$ derived from the dissociation energy of the neutral dimer[47] and the small shift of the adiabatic ionization potential upon complexation ($\approx 27\ cm^{-1}$)[48] is probably too low, because of an erroneous determination of the adiabatic ionization potential in reference [48].[49]

Table 4. Estimated experimental dissociation energies (D_0 in cm^{-1}, $1\ kJ\,mol^{-1} \approx 83.6\ cm^{-1}$) of π-bound complexes of Ar, N_2, and CH_4 with selected aromatic cations compared with values calculated at the MP2/6-311G(2df,2pd) level (D_e in cm^{-1}).

Cation	Ar		N_2		CH_4	
	D_e	D_0	D_e	D_0	D_e	D_0
$C_6H_7^+$	434		929	≈ 800		≈ 950
$C_6H_6^+$ [a]		< 485[e]		$\approx 330-550$[f]		≈ 1000
c-$C_3H_3^+$ [b]	392		1102	860 ± 170		
$C_6H_6O^+$ [c]	396	535 ± 3	771	750 ± 150		
$C_6H_7N^+$ [d]	454	414 ± 28	742	700 ± 200		

[a] Refs. [8a, d]. [b] Ref. [29] (assuming C bonds rather than π bonds). [c] Refs. [11, 30, 45]. [d] Refs. [9, 31, 46]. [e] Measured for $C_6D_6^+$–Ar. [f] Refs. [47–49], probably in error (see text).

Interestingly, the preferred ligand binding site in clusters composed of aromatic cations and nonpolar ligands depends sensitively on the substitution of acidic functional groups. For example, the most stable $C_6H_6^+$–L[8, 50] and $C_6H_7^+$–L structures appear to have intermolecular π-bonds, whereas complexes of the aniline ($C_6H_7N^+$)[31, 46] and (protonated) phenol cations ($C_6H_{6/7}O^+$)[4, 11, 30, 51] with nonpolar L prefer intermolecular hydrogen bonds to the acidic YH_n group ($YH_n = NH_2$, OH, OH_2). Apparently, the favored binding site depends on the magnitude of the positive partial charge localized on the most acidic proton. For example, in the case of the phenol and aniline cations, the protons of the YH_n group carry a large positive partial charge ($+0.66$ and $+0.48$ e),[46] and the resulting strong electrostatic and inductive forces lead to the preference for hydrogen bonding. On the other hand, the positive charge on the protons of the CH_2 group in $C_6H_7^+$ is rather small ($+0.16$ e), leading to weaker hydrogen bonds and the preference for π bonding.

Astrochemical implications: Protonated polycyclic aromatic hydrocarbon molecules are important ions in modern astrochemical models.[15] In particular, they are discussed as possible carriers for some of the well known but as yet unassigned diffuse interstellar bands (DIBs) as well as the unidentified IR emission bands (UIR).[15b, 22] The recent identification of benzene in interstellar objects supports the suggestion of the presence of (protonated) aromatic molecules in interstellar environments.[22] To compare astronomical observations with laboratory data, gas-phase spectra of protonated aromatic hydrocarbon molecules are required. However, such spectra have not been available so far. Consequently, the presented $C_6H_7^+$–L_n spectra, approximating to a high degree the IR spectrum of $C_6H_7^+$, allow us for the first time to test whether or not protonated aromatic hydrocarbon molecules may contribute to the UIR bands. It may be expected that the IR spectra of related protonated polycyclic aromatic hydrocarbon molecules in the C–H stretch range are similar in appearance to the spectrum of protonated benzene. For example, test calculations for protonated naphthalene (protonation at the 2-position) show that the frequencies and IR intensities of the C–H stretch fundamentals are very similar to those of $C_6H_7^+$.

The 3 μm range of the UIR spectrum is dominated by the intense 3.29 μm band ($3040\ cm^{-1}$), which is attributed to aromatic C–H stretch fundamentals.[52] Further (and usually) weaker satellite bands are observed at 3.40 (2940), 3.46 (2890), 3.51 (2850), and 3.56 μm ($2810\ cm^{-1}$), and their interpretation is less certain.[52] According to the $C_6H_7^+$ spectrum deduced in the present work, the mid-IR spectra of small protonated aromatic hydrocarbon molecules are expected to be dominated by intense aliphatic C–H stretch fundamentals of the CH_2 group near $2800\ cm^{-1}$ and possibly a C–C stretch overtone near $2820\ cm^{-1}$. Weak aromatic C–H stretch absorptions should occur in the $3080-3110\ cm^{-1}$ range and may be expected to become more intense as the size of the molecule increases. The comparison between the UIR and $C_6H_7^+$ spectra clearly indicates that protonated benzene provides at most only a minor contribution to the astronomical UIR spectrum. To further test whether larger protonated aromatic hydrocarbon molecules can account for the UIR and DIB bands, laboratory IR and UV-visible spectra are required for these species. The present experimental approach has proven to be a promising tool to obtain such spectra.

Conclusion

IR spectroscopy and quantum chemical calculations have been employed for the first time to probe the interaction of protonated benzene with weakly bound ligands. IRPD spectra of a variety of $C_6H_7^+$–L_n complexes in the C–H stretch range are consistent with a σ complex of $C_6H_7^+$ as the core ion. They confirm that the σ complex of protonated benzene is more stable than the π complex. Hence, the proton differs

principally from larger "spherical" closed shell ions, such as alkali metal ions or ammonium, which apparently form π complexes rather than σ complexes.[53] The stronger cation–π interactions in the latter systems probably arise from the larger size and polarizability of the cation (relative to H^+). The recorded IRPD spectra of $C_6H_7^+$–L_n are nearly independent of L and *n* and thus provide a good approximation to the IR spectrum of isolated $C_6H_7^+$. The spectra and the calculations confirm that the microsolvation with nonpolar solvents has little influence on the properties of the benzenium ion. The deduced IR spectrum of $C_6H_7^+$ provides the opportunity to identify this important ion in fundamental chemical reaction mechanisms (including proton transfer and aromatic substitution) as well as hydrocarbon plasmas. Comparison with the astronomical UIR spectrum demonstrates that $C_6H_7^+$ provides at most only a minor contribution. In addition to the IRPD spectra, calculations of the intermolecular potential of $C_6H_7^+$–Ar and $C_6H_7^+$–N_2 suggest that aromatic hydrocarbon cations prefer intermolecular π bonds to nonpolar ligands over hydrogen bonds. A preliminary spectrum of $C_6H_7^+$–H_2O indicates that this ion–dipole complex is at least a local minimum on the potential of the protonated benzene–water dimer, $[C_6H_6$–$H_2O]H^+$. Future spectroscopic and theoretical studies of $[C_6H_6$–$(H_2O)_n]H^+$ will shed further light on the protonation process of this important model system and the chemical properties of protonated aromatic molecules in polar solvents.

Acknowledgement

This study is part of project No. 20-63459.00 of the Swiss National Science Foundation. O.D. is supported by the Deutsche Forschungsgemeinschaft with a Heisenberg Fellowship (729/1-1). The authors thank R. V. Olkhov for initial experimental studies on $C_6H_7^+$–$(CH_4)_n$ clusters.

[1] a) J. March, *Advanced Organic Chemistry: Reactions, Mechanisms, and Structure*, Wiley, New York, **1992**; b) F. A. Carey, R. J. Sundberg, *Advanced Organic Chemistry*, Plenum, New York, **1995**; c) G. A. Olah, *Acc. Chem. Res.* **1971**, *4*, 240.
[2] a) S. Fornarini, M. E. Crestoni, *Acc. Chem. Res.* **1998**, *31*, 827; b) S. Fornarini, *Mass Spectrom. Rev.* **1997**, *15*, 365; c) D. Kuck, *Mass Spectrom. Rev.* **1990**, *9*, 583; d) B. Chiavarino, M. E. Crestoni, C. H. DePuy, S. Fornarini, R. Gareyev, *J. Phys. Chem.* **1996**, *100*, 16201; e) R. S. Mason, C. M. Williams, P. D. J. Anderson, *J. Chem. Soc. Chem. Commun.* **1995**, 1027.
[3] N. Solcà, O. Dopfer, *Angew. Chem.* **2002**, *114*, 3781; *Angew. Chem. Int. Ed.* **2002**, *41*, 3628.
[4] N. Solcà, O. Dopfer, *Chem. Phys. Lett.* **2001**, *342*, 191.
[5] a) N. Solcà, O. Dopfer, *Angew. Chem.* **2003**, *115*, 1575; *Angew. Chem. Int. Ed.* **2003**, *42*, 1537; b) N. Solcà, O. Dopfer, *J. Am. Chem. Soc.* **2003**, *125*, 1421
[6] E. J. Bieske, O. Dopfer, *Chem. Rev.* **2000**, *100*, 3963.
[7] M. Okumura, L. I. Yeh, J. D. Myers, Y. T. Lee, *J. Phys. Chem.* **1990**, *94*, 3416.
[8] a) O. Dopfer, R. V. Olkhov, J. P. Maier, *J. Chem. Phys.* **1999**, *111*, 10754; b) A. Fujii, E. Fujimaki, T. Ebata, N. Mikami, *J. Chem. Phys.* **2000**, *112*, 6275; c) J. M. Bakker, R. G. Satink, G. von Helden, G. Meijer, *Phys. Chem. Chem. Phys.* **2002**, *4*, 24; d) R. G. Satink, H. Piest, G. von Helden, G. Meijer, *J. Chem. Phys.* **1999**, *111*, 10750.
[9] H. Piest, G. von Helden, G. Meijer, *J. Chem. Phys.* **1999**, *110*, 2010.
[10] a) R. V. Olkhov, O. Dopfer, *Chem. Phys. Lett.* **1999**, *314*, 215; b) S. A. Nizkorodov, D. Roth, R. V. Olkhov, J. P. Maier, O. Dopfer, *Chem. Phys. Lett.* **1997**, *278*, 26.
[11] N. Solcà, O. Dopfer, *J. Phys. Chem. A* **2001**, *105*, 5637.
[12] P. J. Linstrom, W. G. Mallard, *NIST Chemistry WebBook*, NIST Standards and Technology, Gaithersburg MD, 20899 (http://webbook.nist.gov), **2001**.
[13] a) A. B. Fialkov, J. Dennebaum, K. H. Homann, *Combust. Flame* **2001**, *125*, 763; b) A. B. Fialkov, K. H. Homann, *Combust. Flame* **2001**, *127*, 2076; c) K. H. Homann, *Angew. Chem.* **1998**, *110*, 2572; *Angew. Chem. Int. Ed.* **1998**, *37*, 2434.
[14] C. N. Keller, V. G. Anicich, T. E. Cravens, *Planet. Space Sci.* **1998**, *46*, 1157.
[15] a) D. Smith, *Chem. Rev.* **1992**, *92*, 1473; b) T. Snow, V. Le Page, Y. Keheyan, V. M. Bierbaum, *Nature* **1998**, *391*, 259; c) D. K. Bohme, *Chem. Rev.* **1992**, *92*, 1487; d) V. Le Page, Y. Keheyan, T. P. Snow, V. M. Bierbaum, *Int. J. Mass Spectrom.* **1999**, *185–187*, 949.
[16] a) M. N. Glukhovtsev, A. Pross, A. Nicolaides, L. Radom, *J. Chem. Soc. Chem. Commun.* **1995**, 2347; b) Z. B. Maksic, B. Kovacevic, A. Lesar, *Chem. Phys.* **2000**, *253*, 59; c) R. Sumathy, E. S. Kryachko, *J. Phys. Chem. A* **2002**, *106*, 510, and references therein.
[17] Although many other less stable $C_6H_7^+$ isomers exist,[55] they are not considered further because they do not have a six-membered ring and therefore are not produced by the present experimental procedure.
[18] a) G. A. Olah, J. S. Staral, G. Asencio, G. Liang, D. A. Forsyth, G. D. Mateescu, *J. Am. Chem. Soc.* **1978**, *100*, 6299; b) Y. Okami, N. Nanbu, S. Okuda, S. Hamanaka, M. Ogawa, *Tetrahedron Lett.* **1972**, *51*, 5259; c) T. Xu, D. H. Barich, P. D. Torres, J. F. Haw, *J. Am. Chem. Soc.* **1997**, *119*, 406; d) C. A. Reed, N. L. P. Fackler, K. C. Kim, D. Stasko, D. R. Evans, P. D. W. Boyd, C. E. F. Rickard, *J. Am. Chem. Soc.* **1999**, *121*, 6314; e) H. H. Perkampus, E. Baumgarten, *Angew. Chem.* **1964**, *76*, 965; *Angew. Chem. Int. Ed. Engl.* **1964**, *3*, 776.
[19] D. Stasko, C. A. Reed, *J. Am. Chem. Soc.* **2001**, *124*, 1148.
[20] a) B. S. Freiser, J. L. Beauchamp, *J. Am. Chem. Soc.* **1976**, *98*, 3136; b) B. S. Freiser, J. L. Beauchamp, *J. Am. Chem. Soc.* **1977**, *99*, 3214.
[21] For example, the difference between the *σ* complex of $C_6H_7^+$ and the bridged structure (i.e., the lowest transition state) is of the order of 25–45 kJ mol^{-1}.
[22] J. Cernicharo, A. M. Heras, A. G. G. M. Tielens, J. R. Pardo, F. Herpin, M. Guelin, L. B. F. M. Waters, *Astrophys. J.* **2001**, *546*, L123.
[23] S. A. Nizkorodov, O. Dopfer, T. Ruchti, M. Meuwly, J. P. Maier, E. J. Bieske, *J. Phys. Chem.* **1995**, *99*, 17118.
[24] a) F. Pauzat, D. Talbi, M. D. Miller, D. J. DeFrees, Y. Ellinger, *J. Phys. Chem.* **1992**, *96*, 7882; b) D. M. Hudgins, L. J. Allamandola, *J. Phys. Chem.* **1995**, *99*, 8978.
[25] G. Guelachvili, K. N. Rao, *Handbook of Infrared Standards*, Academic Press, London, **1993**.
[26] Gaussian 98 (Revision A.7), M. J. Frisch, G. W. Trucks, H. B. Schlegel, G. E. Scuseria, M. A. Robb, J. R. Cheeseman, V. G. Zakrzewski, J. A. Montgomery, R. E. Stratmann, J. C. Burant, S. Dapprich, J. M. Millam, A. D. Daniels, K. N. Kudin, M. C. Strain, O. Farkas, J. Tomasi, V. Barone, M. Cossi, R. Cammi, B. Mennucci, C. Pomelli, C. Adamo, S. Clifford, J. Ochterski, G. A. Petersson, P. Y. Ayala, Q. Cui, K. Morokuma, D. K. Malick, A. D. Rabuck, K. Raghavachari, J. B. Foresman, J. Cioslowski, J. V. Ortiz, B. B. Stefanov, G. Liu, A. Liashenko, P. Piskorz, I. Komaromi, R. Gomperts, R. L. Martin, D. J. Fox, T. Keith, M. A. Al-Laham, C. Y. Peng, A. Nanayakkara, C. Gonzalez, M. Challacombe, P. M. W. Gill, B. G. Johnson, W. Chen, M. W. Wong, J. L. Andres, M. Head-Gordon, E. S. Replogle, J. A. Pople, Gaussian, Inc., Pittsburgh, PA, **1998**.
[27] S. F. Boys, F. Bernardi, *Mol. Phys.* **1970**, *19*, 553.
[28] a) A. D. Buckingham, *Adv. Chem. Phys.* **1967**, *12*, 107; b) C. G. Gray, K. E. Gubbins, *Theory of Molecular Fluids, Vol. 1*, Clarendon, Oxford, **1984**.
[29] a) D. Roth, O. Dopfer, *Phys. Chem. Chem. Phys.* **2002**, *4*, 4855; b) O. Dopfer, D. Roth, J. P. Maier, *Int. J. Mass. Spectrom.* **2002**, *218*, 281; c) O. Dopfer, D. Roth, J. P. Maier, *J. Am. Chem. Soc.* **2002**, *124*, 494.
[30] a) N. Solcà, O. Dopfer, *Chem. Phys. Lett.* **2000**, *325*, 354; b) N. Solcà, O. Dopfer, *J. Mol. Struct.* **2001**, *563/564*, 241.
[31] N. Solcà, O. Dopfer, *J. Phys. Chem. A* **2002**, *106*, 7261.
[32] E. P. L. Hunter, S. G. Lias, *J. Phys. Chem. Ref. Data* **1998**, *27*, 413.
[33] O. Dopfer, *J. Phys. Chem. A* **2000**, *104*, 11693.
[34] a) N. Solcà, O. Dopfer, *Chem. Phys. Lett.* **2001**, *347*, 59; b) M. Miyazaki, A. Fujii, T. Ebata, N. Mikami, *Chem. Phys. Lett.* **2001**, *349*, 431.

[35] E. Venuti, L. Halonen, R. G. Della Valle, *J. Chem. Phys.* **1999**, *110*, 7339.
[36] E. T. White, J. Tang, T. Oka, *Science* **1999**, *284*, 135.
[37] a) D. W. Boo, Z. F. Liu, A. G. Suits, J. S. Tse, Y. T. Lee, *Science* **1995**, *269*, 57; b) D. W. Boo, Y. T. Lee, *Chem. Phys. Lett.* **1993**, *211*, 358; c) D. W. Boo, Y. T. Lee, *J. Chem. Phys.* **1995**, *103*, 520; d) D. W. Boo, Y. T. Lee, *Int. J. Mass. Spectrom. Ion Processes* **1996**, *159*, 209.
[38] a) S. N. Thakur, L. Goodman, A. G. Ozkabak, *J. Chem. Phys.* **1986**, *84*, 6642; b) T. A. Stephenson, P. L. Radloff, S. A. Rice, *J. Chem. Phys.* **1984**, *81*, 1060.
[39] Frequency calculations of dimers are carried out at the MP2/6-31 G* level.
[40] E. S. Kryachko, M. T. Nguyen, *J. Phys. Chem. A* **2001**, *105*, 153.
[41] Collision-induced dissociation is achieved by introducing 10^{-5} mbar of He in the octopole. The average center-of-mass collision energy is of the order of 0.2 eV.
[42] The effective temperature of a cluster in a molecular beam is (partly) determined by the dissociation energy of the most weakly bound ligand. The larger the intermolecular bond strength of this ligand, the more internal energy can be stored in the complex (before cooling through evaporation processes will become effective).
[43] a) M. Miyazaki, A. Fujii, T. Ebata, N. Mikami, *Phys. Chem. Chem. Phys.* **2003**, 1137; b) K. Kleinermanns, C. Janzen, D. Spangenberg, M. Gerhards, *J. Phys. Chem. A* **1999**, *103*, 5232; c) T. Ebata, A. Fujii, N. Mikami, *Int. Rev. Phys. Chem.* **1998**, *17*, 331.
[44] a) R. V. Olkhov, S. A. Nizkorodov, O. Dopfer, *Chem. Phys.* **1998**, *239*, 393; b) O. Dopfer, R. V. Olkhov, J. P. Maier, *J. Phys. Chem. A* **1999**, *103*, 2982; c) O. Dopfer, D. Roth, J. P. Maier, *J. Phys. Chem. A* **2000**, *104*, 11702; O. Dopfer, N. Solca, R. V. Olkhov, J. P. Maier, *Chem. Phys.* **2002**, *283*, 85.
[45] C. E. H. Dessent, S. R. Haines, K. Müller-Dethlefs, *Chem. Phys. Lett.* **1999**, *315*, 103.
[46] N. Solcà, O. Dopfer, *Eur. Phys. J. D* **2002**, *20*, 469.
[47] a) R. Nowak, J. A. Menapace, E. R. Bernstein, *J. Chem. Phys.* **1988**, *89*, 1309; b) P. Hobza, O. Bludsky, H. L. Selzle, E. W. Schlag, *J. Chem. Phys.* **1993**, *98*, 6223; c) B. Ernstberger, H. Krause, H. J. Neusser, *Z. Phys. D.* **1991**, *20*, 189.
[48] H. Shinohara, S. Sato, K. Yoshihara, K. Kimura, *J. Electron Spectrosc. Relat. Phenom.* **1998**, *88–91*, 131.
[49] The adiabatic ionization potential of C_6H_6–N_2 is probably not observed in the photoelectron spectrum reported in ref. [48] due to a large geometry change upon ionization (leading to vanishing Franck-Condon factors for transitions near the adiabatic ionization potential.
[50] K. Siglow, R. Neuhauser, H. J. Neusser, *J. Chem. Phys.* **1999**, *110*, 5589.
[51] A. Fujii, M. Miyazaki, T. Ebata, N. Mikami, *J. Chem. Phys.* **1999**, *110*, 11125.
[52] a) T. R. Geballe, T. H. Lacy, S. E. Persson, P. J. McGregor, B. T. Soifer, *Astrophys. J.* **1985**, *292*, 500; b) L. J. Allamandola, A. G. G. M. Tielens, J. R. Barker, *Astrophys. J. Suppl. Ser.* **1989**, *71*, 733; c) C. Joblin, *Faraday Discuss.* **1998**, *109*, 349; M. P. Bernstein, S. A. Sandford, L. J. Allamandola, *Astrophys. J.* **1996**, *472*, L127.
[53] J. C. Ma, D. A. Dougherty, *Chem. Rev.* **1997**, *97*, 1303.
[54] N. Solcà, PhD thesis, University of Basel (Switzerland), **2003**.
[55] S. G. Lias, P. Ausloos, *J. Chem. Phys.* **1985**, *82*, 3613.

Received: December 2, 2002 [F4629]

